National Conference with International Participation

ENGINEERING MECHANICS 2008

Svratka, Czech Republic, May 12 – 15, 2008

# EXPERIMENTAL STUDY OF WIND LOAD ON RAILWAY-STATION OBEJCTS

**D. Zachoval[*] , M. Jirsák [**]**

**Summary:** *The case-study of wind load on innovation railway-station objects was performed using VZLÚ boundary layer wind tunnel. The results of this experiment were processed to mean values, its standard deviations and to the gust peak factors. Spectral analysis of this signal was made for each tap with extreme value of the gust peak factor. Dimensionless values of the pressure coefficient were related to reference dynamic pressure conformable with Eurocode 1.*

## 1. Introduction

The paper outlines case-study of wind load acting on low-rise railway-station roofs. The innovation is concerned of new roof structure over the railway-station platforms. Structural analysis of the railway-station roofs uses a code for the wind load assessment. The code includes parameters of wind flow above the flat uniformly rough terrain (FUR) without specific buildings. As the railway station finds in city center of Salzburg (with substantially higher buildings in near vicinity), oncoming flow structure differs significantly with wind direction.

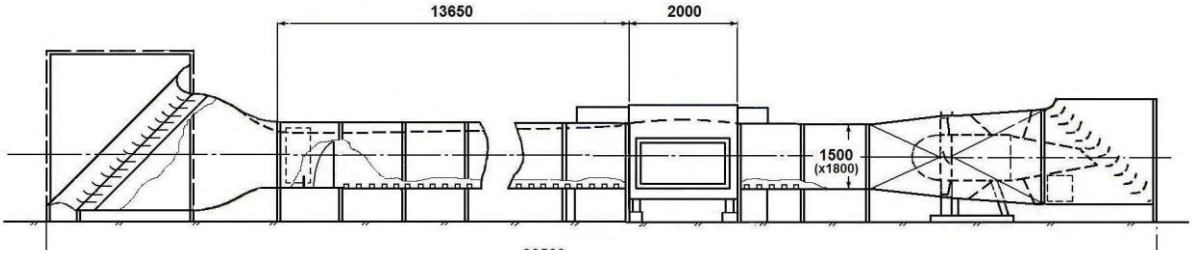


Fig. 1: Boundary Layer Wind Tunel of VZLÚ a.s.

The real wind structures oncoming to the objects was simulated in the boundary layer wind tunnel as equilibrium flow over FUR terrain with roughness length 1.17 m (the roughness field with 40 mm cubes). Into the model near estate was included area with diameter 1000 m around the railway-station. The wind load on the structures was investigated for 16 wind directions and the maximum wind load was found over all wind directions. It was illustrated as an envelope surface of isosurface for all individual wind azimuths over the roof structure.

[*] Mgr. David Zachoval, : Aeronautical Research and Test institute (VZLÚ a.s.); Beranových 130; 199 05 Praha; tel.: +420 225 115 513, fax: +420 296 920 518; e-mail: zachoval@vzlu.cz

[**] Ing. Milan Jirsák, CSc.: Aeronautical Research and Test Institute (VZLÚ a.s.); Beranových 130; 199 05 Praha; tel.: +420 225 115 530, fax: +420 296 920 518; e-mail: jirsak@vzlu.cz

## 2. The Atmospheric Boundary Layer (ABL) simulation

The simulation of ABL in the wind tunnel (see Fig. 1) above the terrain with urban roughness for this experiment uses the roughness field in net fetch of 11.4 m. The Counihan vortex generator is situated in front of the roughness field composed from battery of elliptic knives in combination with castellated wall.

Boundary layer properties were tested over the section of 700 mm upwind the end of cube fetch. The vertical distribution of mean velocity and turbulence intensity were checked above centre of turntable and in lateral distance ±600 mm from it. The Fig. 2 introduces these mean velocity and the standard deviation profiles normalized by friction velocity ($U/u^*$ and $u/u^*$).

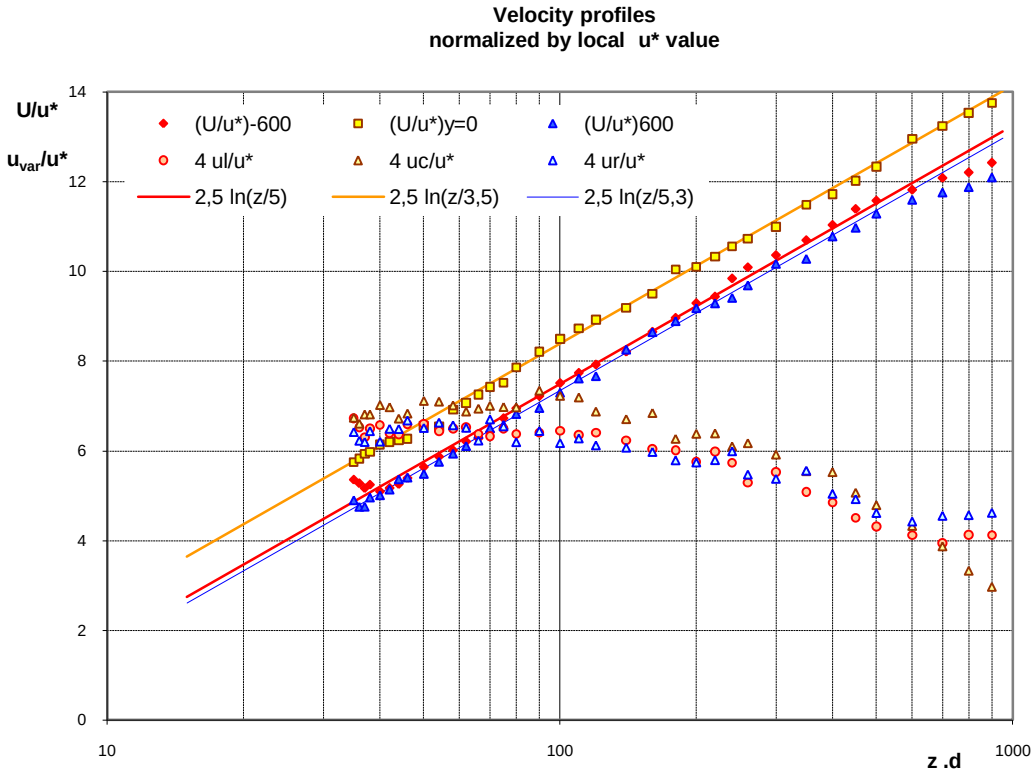


Fig. 2: Incident flow

Span average value of model roughness length $z_{0,m}$ = 4.7 mm derived from the three vertical velocity profiles is appropriate to roughness length $z_0$ = 1.17 m in full scale.

Power spectrum in Fig. 3 monitors the distribution of turbulent energy (that of longitudinal component) in dependence on the dimensionless frequency as result of the FFT processing. The region of power dependence on frequency is exhibited, proper to inertial sub-range,

showing energy equilibrium state of the boundary layer.

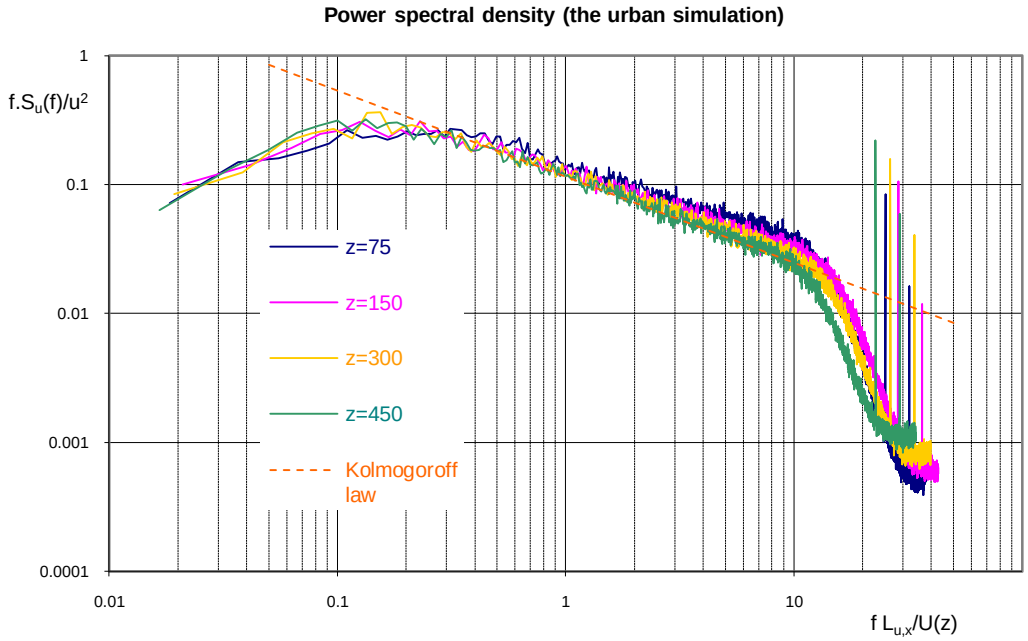


Fig. 3: Power spectral density, $L_{u,x}$ is integral length scale of turbulence

## 3. Model of the railway-station

The model (VZLÚ production) was designed according the customer data (transferred to convenient software), complied with available satellite pictures. The passive estate members were machined from synthetic wood while R.S. roofs were manufactured as carbon fibre composite.

Fig. 4: Model of the Salzburg railway-station with surrounding estate

The pressure taps (218 pieces) were disposed over the upper and lower roof surfaces and connected with pressure scanner Easterline (model 16TC, range ±10”WC) by polyethylene tubing within inner diameter of 1 mm and 800 mm length. The frequency response of the measuring line (see Fig. 8) was measure, which was used later for signal coerrection at its processing. It was measured as the response of the line to the pressure pulse with very short duration (approximately 2 ms).

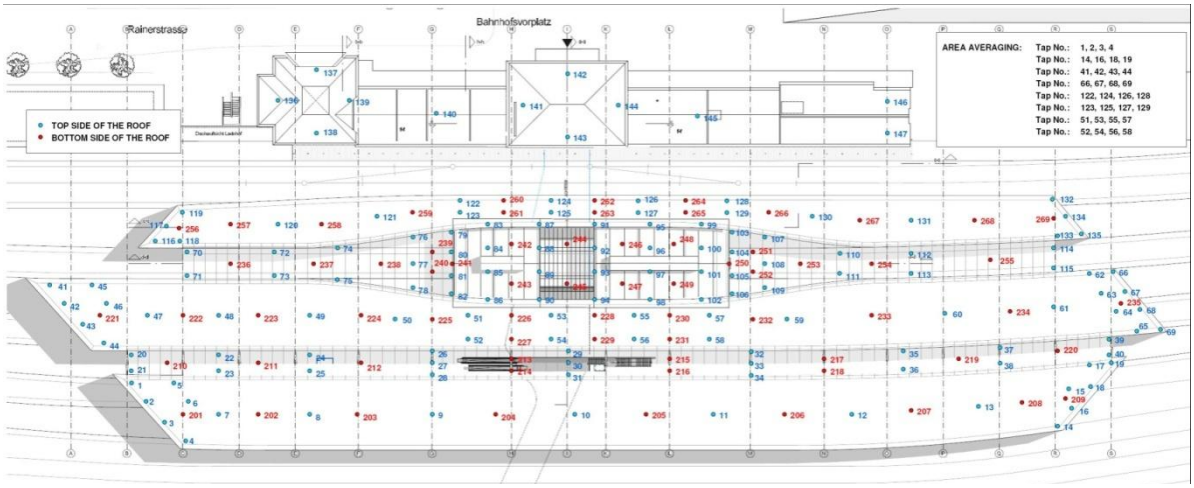


Fig. 5: Numbering of the pressure taps on bottom and top site of the roof structure

## 4. Set of the equipment

The signals were sampled with frequency 3kHz during time period 30 s each pressure tap and it were filtered by low-pass analogue filter with limit frequency approximately 290 Hz.

## 5. The similarity criteria

The modeled case is clearly confined to the *atmospheric surface layer* range whose structure the wind tunnel is able to product quite consistently. Thickness of the ASL (roughly 15% of ABL) represents lower 70÷100 m layer where shear stress distribution is nearly constant as follows from the ASL definition. All the well-known characteristics of ASL over flat uniformly rough terrain are valid only on heights overcoming tops of roughness elements, forming its statistical planar homogeneity.

Existence of the "fully rough turbulent flow" (it is always present in the atmosphere) is conditioned in BL wind tunnel by sufficient velocity with respect to magnitude of roughness elements. The similarity is attained at sufficient value of "roughness Reynolds number" Re*

$$Re^* = \frac{u^* z_0}{\nu} > Re_k^*, \text{ where} \qquad (1)$$

u* .. is friction velocity, $z_0$ .. roughness length and ν .. is kinematic viscosity. Taking critical value of $Re_k^* \approx 2{,}5$ (ASCE man. 1969) and our mean $z_0$ = 4.7 mm and $u^*/U_G \approx 0{,}0674$ we get

$$u^* > 2.5\frac{15}{4.7E-3} = 0.00798\,m/s \text{ whence } U_G > 0{,}184\ m/s.$$

The requirement is ample satisfied with actual experimental value of the gradient velocity $U_G \approx$ 15 m/s.

## 6. Results

The pressure values on both sides of the roof structure were measured as different pressure $\Delta p_i$ between the wind pressure at the $i$-tap on the roof structure $p_{w,i}$ and the static pressure in the wind tunnel $p_{stat}$.

$$\Delta p_i = p_{w,i} - p_{stat} \tag{2}$$

The static pressure was taken from the Prandtl probe static orifice, situated above the boundary layer upwind the model section of the wind tunnel.

There were several problems. At first, reference static pressure in relatively smooth flow above the boundary layer is different from that in very disturbed flow in the boundary layer bottom. In the consequence, the sign of resulting pressure coefficients was mostly negative. This dificult was removed expressing the differences between upper and lower roof surface.

$$p_i = \Delta p_{i,lower} - \Delta p_{i,upper}\,, \tag{3}$$

where $p_i$ represents force at the $i$ upper pressure taps. The forces ensuing from positive value of $p_i$ pulls the roof structure up and force ensuing from negative value of $p_i$ pushes the roof down.

The results of the wind load measurement were mean pressure coefficients $\bar{c}_{p,i}$. It is defined as ratio

$$\bar{c}_{p,i} = \frac{\bar{p}_i}{q_{ref}} \tag{4}$$

where $q_{ref}$ is reference dynamic pressure. It was request to of compare the experimental dimensionless results with the values developed from codes related to wind at the height of 10 m above earth. Therefore the value of dynamic head on height of z = 40 mm developed from the scaled profile of mean velocity of incident flow. $U_{ref}$ = 6.09 m/s i.e. $q_{ref} \approx 21.45$ Pa was used for the pressure coefficient $c_{p,i}$ final evaluation.

The statistical processing of the pressure signal gave to following values of the pressure. Mean pressure $\bar{p}_i$, its standard deviation $p_{i,SD}$, maximum $\hat{p}_i$ and minimum peak $\check{p}_i$ of the pressure signal.

Spectral analysis of the pressure signal was done in the case when the its negative peak was at least four times higher than its standard deviation.

It is ensuing from equation

$$\check{p}_i = \bar{p}_i + g p_{i,SD} \Rightarrow g = \frac{\check{p}_i - \bar{p}_i}{p_{i,SD}} \tag{5}$$

where $g$ is gust peak factor.

The maximum wind load on roof structure is depicted in Fig. 6 as an envelope of the wind loads proper to all measured wind directions.

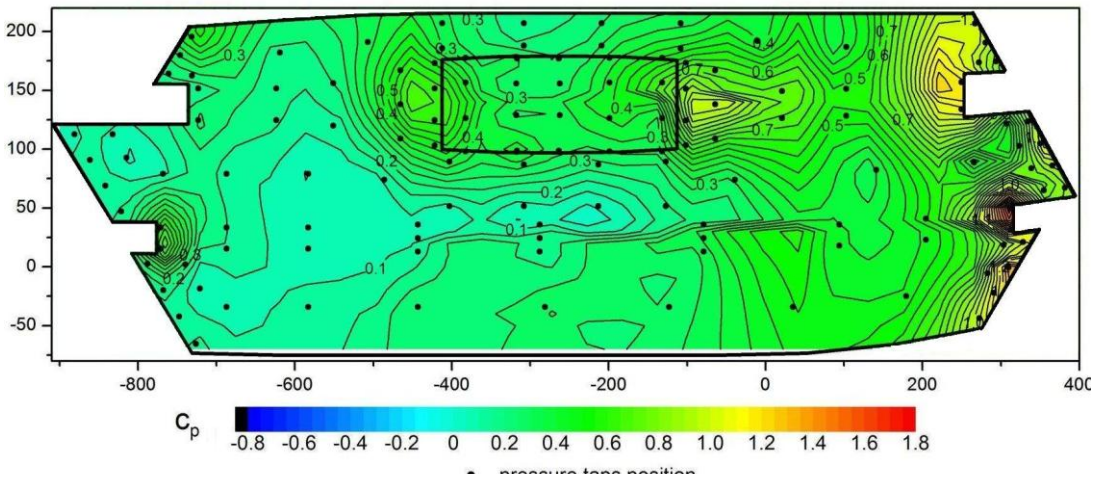


Fig. 6: maximum wind load on roof structure, the positive value of the cp represents the suction

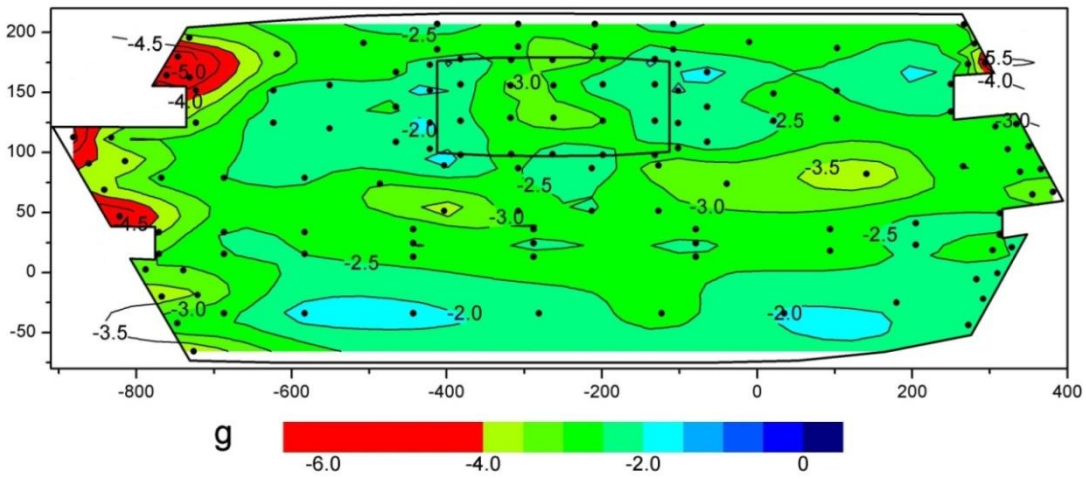


Fig. 7: Gust peak factor, for maximum wind loading pressure coeficinets

Examples of pressure spectra are in Fig. (9 – 12). The examples were chosen for the peak factors proper to the maximal wind acting on the structure. The pressure spectra were prepared for the all records where $|g| \geq 4$. Spectra of the particular cases are labelled by proper angle/tap combination. Here it should mention occurrence of the disturbing peaks caused either by standing acoustic waves in the wind channel, or to the frequencies induced by four fan blades.

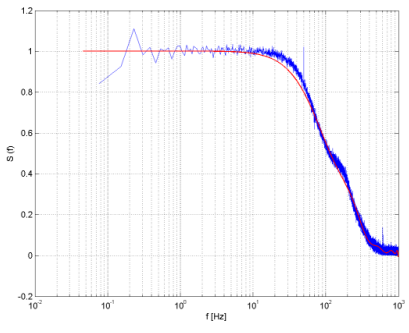

Fig. 8: Response of the measuring line

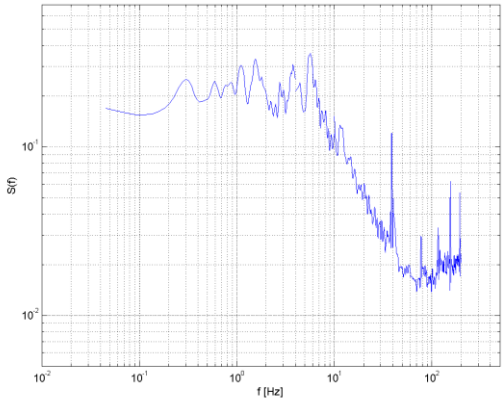


Fig. 9: Spectrum of pressure record on the point 4 (0° wind angle)

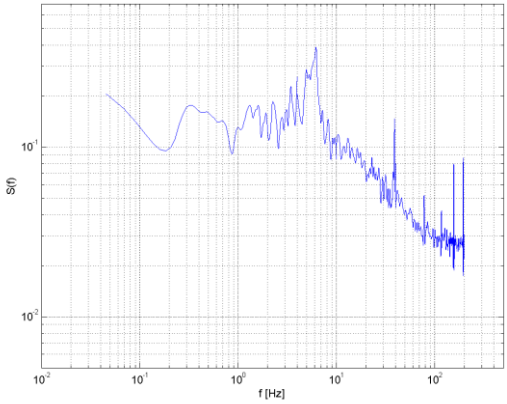


Fig. 10: Spectrum of pressure record on the 135 (225° wind angle)

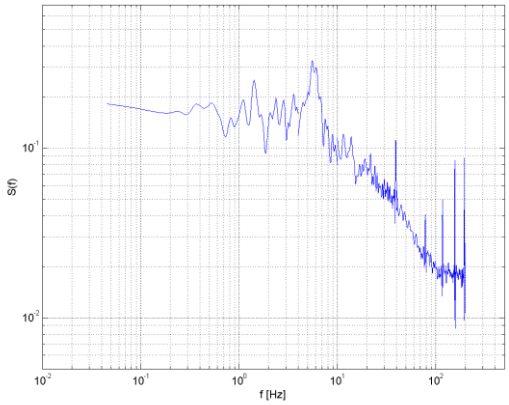


Fig. 11: Spectrum of pressure record on the point 116 (67.5° wind angle)

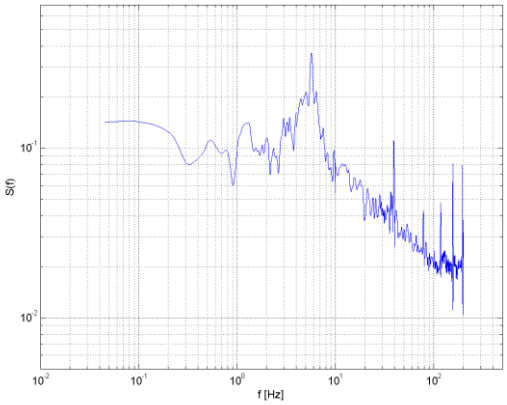


Fig. 12: Spectrum of pressure record on the point 117 (67.5° wind angle)

It is visible that with respect of possible elimination of the disturbing peaks one could accept the spectra to be valid in frequencies approximately from 0.3 Hz up to roughly 100 Hz. This limit of the modeled frequency answers to lower frequency limit in the case of full scale. This follows from Strouhal number similarity:

$$Sh = \frac{f_m L_m}{(U_G)_m} = \frac{f_{FS} L_{FS}}{(U_G)_{FS}}. \quad (6)$$

At the actual length scale $L_m/L_{FS}$ = 1/205 and supposed $(U_G)_m/(U_G)_{FS}$ = 1/5 for strong wind, we get

$$(f_{FS})_{max} = (f_m)_{max} \frac{L_m}{L_{FS}} \frac{(U_G)_{FS}}{(U_G)_m} = 100 \frac{1}{250} 5 = 2Hz. \quad (7)$$

Variability of the spectral distribution of fluctuating energy for the individual taps of this spectra measurement is evident.

## 7. Pressure results and their discussion

Resulting pressure coefficients $c_{p,i}$ as they were measured on the taps are found within range form -0,62 to 1.76. Their values are importantly influenced by estate environs, depending on wind angle as it is documented by following:

Surveying Fig. 6 we can see that the maximal positive pressure differences (acting upwards) appear on northern ends of platform roofs at angles of about 247.5°, where wind comes from free space above rails (NE wind) and turns up on the roof tips with $c_{p,i}$ approaching the absolute maximum with values of about 1.8 (taps No.39 and 114 found close the cutouts of northern roof tips). The next area of increased positive pressure (lower, about $c_p \approx 1.2$) is found near the front part of the hall ridge appearing at wind angles of 202.5°.

The points with high gust peak factor are just at the ends of the roof structure. The wind can flutter with the roof structure. Critical dynamic load will occur when frequency of the flutter approaches the natural frequency of the roof structure.

## 8. Conclusions

Experiments focused on wind load acting on the low railway-station objects which are submerged in the higher surrounding buildings represent very demanding task with respect of quite different oncoming wind structure coming from different wind angles, mostly containing wakes of near buildings which changes mean static pressure on the site. Another complication following Salzburg railway-station modelling arises in the consequence of surrounding orography, causing difficulties in connecting of wind tunnel results with meteorological statistics measured on site of Salzburg airport much less affected by orography effects. Simulated wind approached the complete model from flat uniformly rough terrain (its structure) was modified only by passive building environs. In the sense, assessment of actual wind loading on the parts of railway-station structure, as well as the approach of pedestrian wind conditions are valid, of course, without directional changes of the gradient velocity caused by the orography.

The experimental assessment of the wind loading on complex roof structure is important because the code includes just basic shape of the roofs and just two basic wind directions. The code calculated with wind coming from flat uniformly rough terrain and it doesn't include specific estate at vicinity of the measured object.

The complete wind tunnel model with the modelled neighbouring estate (from aside the FUR simulation) solves the tasks of dynamic wind acting on railway-station objects with much higher accuracy and fine details than it would do the wind codes, so as then any CFD model.

## References

ASCE Manuals & Reports on Eng. Practice, No.67 (1999) Wind Tunnel Studies of Buildings, American Society of Civil Engineers, Reston, Virginia.

Claës Dyrbye, Svend O. Hansen (1996), Wind Load on Structures, Original published in Danish.

ČSN EN 1991-1-4 Zásady navrhování a zatížení konstrukcí – Část 2-4 Zatížení konstrukcí – Zatížení větrem

Jirsák M., Zachoval D.: Experimental study on innovation project of Salzburg railway station, VZLÚ, R 4152/07

Rep. VZLÚ V-1708/2000 Jirsak M. et al.: The completing of the simulation development (Project MPO FB-C/85/99 RC1.6, in Czech)